



HAL
open science

Mechanical properties of ferrofluid applications: centering effect and capacity of a seal

Romain Ravaud, Guy Lemarquand, Valérie Lemarquand

► **To cite this version:**

Romain Ravaud, Guy Lemarquand, Valérie Lemarquand. Mechanical properties of ferrofluid applications: centering effect and capacity of a seal. *Tribology International*, 2009, 43 (1-2), pp.76-82. 10.1016/j.triboint.2009.04.050 . hal-00392784

HAL Id: hal-00392784

<https://hal.science/hal-00392784>

Submitted on 9 Jun 2009

HAL is a multi-disciplinary open access archive for the deposit and dissemination of scientific research documents, whether they are published or not. The documents may come from teaching and research institutions in France or abroad, or from public or private research centers.

L'archive ouverte pluridisciplinaire **HAL**, est destinée au dépôt et à la diffusion de documents scientifiques de niveau recherche, publiés ou non, émanant des établissements d'enseignement et de recherche français ou étrangers, des laboratoires publics ou privés.

Mechanical Properties of Ferrofluid

Applications: Centering Effect and Capacity of a Seal

R. Ravaud, G. Lemarquand^{*}, V. Lemarquand

*Laboratoire d'Acoustique de l'Universite du Maine, UMR CNRS 6613, Avenue
Olivier Messiaen, 72085 Le Mans Cedex 9, France*

Abstract

This paper presents three dimensional study of a ferrofluid seal, its centering effect and its static capacity. Thus, a method based on a potential energy criterion has been put forward to study the seal shape. But such a use of ferrofluid seals is interesting only if the magnetic field created by the permanent magnets saturates totally the ferrofluid. Two cylindrical structures consisting of two and three outer ring permanent magnets with an inner non-magnetic cylinder are considered. The calculation of the magnetic pressure of the ferrofluid seal is analytically established.

Key words: Ferrofluids, Hydrostatic lubrication, Journal bearings

PACS: 47.65 Cb

^{*} Corresponding author.

Email address: guy.lemarquand@univ-lemans.fr (G. Lemarquand).

1 Introduction

A magnetic ferrofluid consists of a stable colloidal suspension of subdomain magnetic particles, $10nm$ in size, in a liquid carrier [1][2]. Each magnetic particle is commonly assimilated to a sphere which is a magnetic dipole. The dipole can be oriented according to the presence of an external magnetic field. Studies on ferrofluids deal either with their chemical and physical properties [3][4] or their mechanical behavior [5][6]. Ferrofluids have various engineering applications [7] and the authors are interested in the design of ironless loudspeakers [8]-[12]. Electromagnetic pumps are designed and studied for the processing industry of liquid metal or for medical applications [13].

Moreover, ferrofluids are also often used as rotating shaft seals and the pioneering work regarding the ferrofluid lubrication was done by Tarapov [14]. Indeed, he considered a plain journal bearing lubricated by ferrofluid and submitted to a non-uniform magnetic field. We can note also that many studies have been carried out on the dynamic behaviors of ferrofluids [15]-[23]. In addition, recent trends in the ferrofluid lubrication applications are described and discussed, taking into account various phenomena including cavitation [24]-[27].

This paper discusses both the centering effect of ferrofluid seals and their static capacity when submitted to large magnetic fields (higher than $400kAm^{-1}$). As ferrofluids are used for sealing applications, we present a method describing a way of optimizing the structure dimensions in order to improve its centering effect, its static capacity as well as its watertightness. Our structure is ironless and the constitutive parts are either made out of permanent magnets

(the stator) or non magnetic materials (the moving part). Consequently, no reluctance effect is observed. The intensity of the magnetic field created by the ring permanent magnets largely saturates the ferrofluid.

Although numerical approaches are commonly used to study ferrofluid seals, the authors feel that three-dimensional analytical approaches allow flexible ways of optimizing ferrofluid seals.

It is emphasized here that such a way of describing ferrofluid seals is possible because the structures considered in this paper are ironless. As such ironless structures are commonly used in industrial or research applications, the method presented in this paper seems to be useful.

2 Structure descriptions

2.1 Notation

The structure considered consists of several outer ring permanent magnets and an inner non-magnetic cylinder. The magnets are stacked and their polarizations are radial, but in opposed directions. Figure 1 presents two examples of ironless structures using permanent magnets and ferrofluid seals. Figure 1-A shows a structure composed of three ring permanent magnets with radial polarizations and an inner non-magnetic piston. Figure 1-B shows a structure composed of two ring permanent magnets with radial and opposite polarizations and an inner non-magnetic piston. The non-magnetic cylinder is assumed to be perfectly centered with the ring permanent magnets. For the rest of this

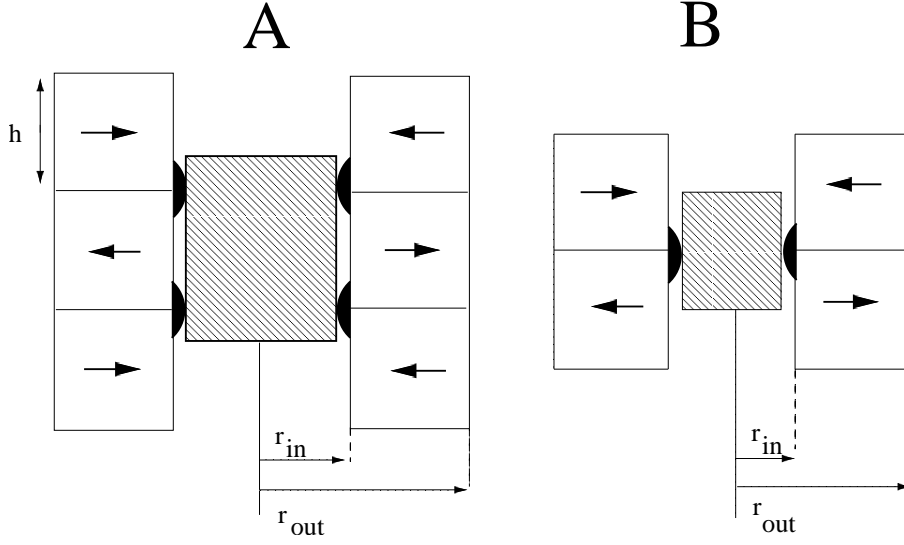


Fig. 1. A: three ring permanent magnets and an inner non-magnetic cylinder with two ferrofluid seals; B: two ring permanent magnets and an inner non-magnetic cylinder with one ferrofluid seal; the ring inner radius is r_{in} , the ring outer radius is r_{out} , the height of a ring permanent magnet is h .

paper, we use the following notations for the description of the ironless structures: the ring inner radius is r_{in} , the ring outer radius is r_{out} and the ring permanent magnet height is h . The z axis is a symmetry axis.

The magnetic field produced by the ring permanent magnets has been determined by using the coulombian model. Consequently, each permanent magnet is represented by two curved charged surfaces. When the vector polarization is directed towards the inner non-magnetic piston, the ring inner face is charged with the magnetic pole surface density $+\sigma^*$ and the ring outer one is charged with the magnetic pole surface density $-\sigma^*$. When the vector polarization is in the opposite direction, the ring inner face is charged with the magnetic pole surface density $-\sigma^*$ and the ring outer one is charged with the magnetic pole surface density $+\sigma^*$.

The accurate knowledge of the magnetic field in the air gap is in fact the crucial point for optimizing ironless permanent magnet topologies with ferrofluid seals submitted to magnetic fields higher than $400kAm^{-1}$. Indeed, the potential energy in the ferrofluid seal is essentially linked to the magnetic energy resulting from the interaction between the magnetic field produced by the ring permanent magnets and the ferromagnetic particles.

It is emphasized here that the expressions of the magnetic field created by ring permanent magnets whose polarization is radial have been determined in a previous paper [28]. We illustrate in the next section where the ferrofluid goes when submitted to the magnetic field produced by two or three ring permanent magnets.

2.2 Magnetic field created by the ring permanent magnets

By using the coulombian model of a magnet, the analytical expressions of the magnetic field [28] are suitable for representing the iso-field lines. The ring inner radius, r_{in} , equals 0.025 m and the permanent magnet height, h , equals 0.003 m. The magnetic pole surface density $+\sigma^*$ equals 1 T.

Figure 2 shows that the magnetic field \mathbf{H} is the strongest near the permanent magnets, especially where the magnetic field gradient is the most important. Such figures are suitable for the design of ironless loudspeaker in which the number of ferrofluid seals has certainly an influence on the dynamic behavior of the emissive piston. In magnetic bearings, it is also useful to determine the quantity of ferrofluid that should be used so as to create one or two ferrofluid seals.

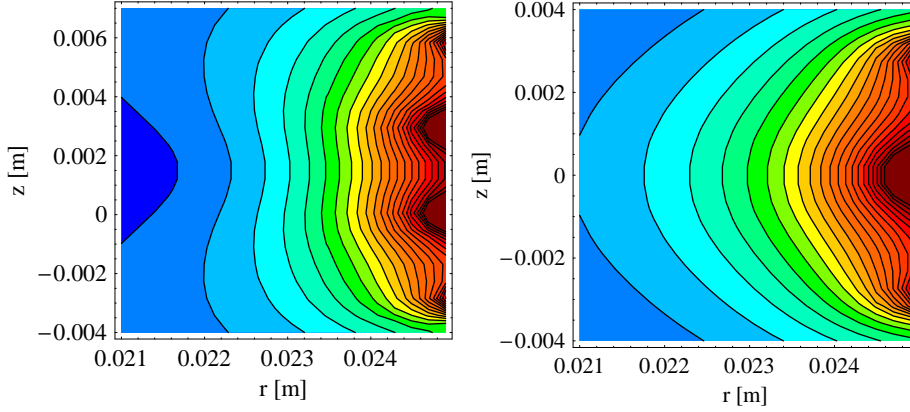


Fig. 2. Magnetic field created by the three (left side)and two (right side) ring permanent magnets. The figure shows a detail view of the region outside the magnets and on the inner side of the device, this zone is $3mm \times 3mm$ square. $r_{in} = 0.025$ m, $h = 0.003$ m, $\sigma^* = 1$ T

2.3 The concept of magnetic pressure

The previous section has presented two examples of ironless structures with ring permanent magnets whose polarization is radial and ferrofluid seals. We discuss now the assumptions taken for defining the concept of magnetic pressure in ferrofluid seals submitted to magnetic fields which saturate the ferrofluid. The most important concept in the design of ironless structures with ferrofluid seals is the knowledge of the regions in space where the ferrofluid goes. Strictly speaking, the magnetic particles are attracted towards the highest intensity regions of the magnetic field. For the proposed configurations, the magnetic field intensity there is greater than 400 kA/m. In addition, we use commercial ferrofluids either from the company Ferrotec or Ferrolabs . Such ferrofluids have a saturation magnetization, M_s , smaller than 32 kA/m and a particle concentration below 5.5% in volume . Therefore, the magnetic field, H , created by the permanent magnets is far higher than the ferrofluid

critical field [29]. So, the ferrofluid is totally saturated and its magnetization is denoted M_s . Moreover, as the ferrofluid is completely saturated, its magnetic permeability is equal to one. Furthermore, the presence of ferrofluid does not modify the field created by the permanent magnets and the field created by the ferrofluid itself is omitted. Thus, all the particles of the saturated ferrofluid are aligned with the permanent magnet orienting field. Consequently, the ferrofluid magnetization has the same direction as the orienting field. In addition, the sedimentation in chains of the ferrofluid particles is omitted [30]. However, it is noted that at laboratory temperature and at rest, the sedimentation phenomenon is observed in the device. Some realistic assumptions are also taken into account: we neglect the thermal energy E_T ($E_T = kT$ where k is Boltzmann's constant and T is the absolute temperature in degrees Kelvin) and the gravitational energy E_G ($E_G = \Delta\rho V g L$ where V is the volume for a spherical particle, L is the elevation in the gravitational field, g is the standard gravity, $\Delta\rho$ is the difference between the ferrofluid density and the outer fluid). In addition, the surface tension exists but when the values of both the surface tension coefficient, A , (A equals $0.0256kg/s^2$ for the used ferrofluids) and the radius of curvature are considered, the effect of the surface tension can be omitted: this latter does not deform the free boundary surface. Eventually, this paper deals with the ferrofluid free boundary surface. Its shape depends on the result of the force competition at this boundary. On one hand, the magnetic pressure, p_m , is exerted. It is given by:

$$p_m(r, z) = \mu_0 \mathbf{M}_s \cdot \mathbf{H}(r, z) = \mu_0 M_s \sqrt{H_r(r, z)^2 + H_z(r, z)^2} \quad (1)$$

where both magnetic field components $H_r(r, z)$ and $H_z(r, z)$ are analytically calculated [31][28]. Finally, for hydrodynamic pressures which equal zero or

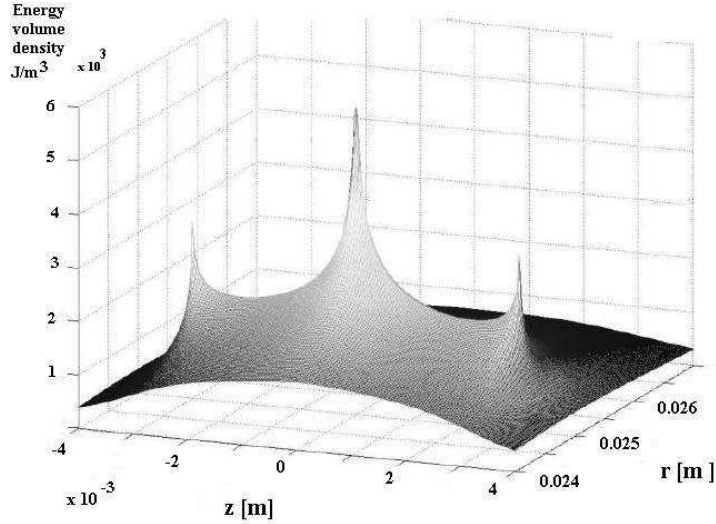


Fig. 3. Three-dimensional representation of the magnetic pressure in front of two ring permanent magnets whose polarizations are radial, but in opposed directions. have low values, the seal free boundary surface is a magnetic iso-pressure surface. Then, its mechanical properties, such as its capacity or its stiffness can be studied.

We represent in Fig 3 a three-dimensional representation of the magnetic pressure created by two ring permanent magnets whose polarizations are radial, but in opposed directions. This magnetic pressure can also be seen as a magnetic energy volume density, and can be expressed either in N/m^2 or in J/m^3 .

The magnetic pressure $p_m(r, z)$ has been determined with (1). Figure 3 shows that the magnetic pressure is greater near the two ring permanent magnets, especially where the magnetic field gradient is the strongest. This region of space corresponds also to the points in which the magnetic field is the strongest. Such a representation is useful for seeing where the magnetic pressure is the greatest. In other words, this representation is interesting because it shows that the potential energy is concentrated in a very small ferrofluid volume. As a

consequence, it gives indications about what quantity of ferrofluid should be used to design a ferrofluid seal. If a large quantity of ferrofluid is used, the ferrofluid seal is thick, the potential energy increases but the viscous effects become an actual drawback according to the dynamic movement of the inner cylinder. If too small an amount of ferrofluid is used, the viscous effects disappear but all the interesting properties of the ferrofluid seal (damping, stability, linearity,...) disappear as well. In short, to a given geometry (here two ring permanent magnets with an inner non-magnetic cylinder) corresponds an adequate quantity of ferrofluid which has some interesting physical properties with very little viscous effects. For the rest of this paper, we use the concept of potential energy for studying the ferrofluid seals. This potential energy is defined by (2):

$$E_m = - \int \int \int_{(\Omega)} p_m(r, z) dV \quad (2)$$

where (Ω) is the ferrofluid seal volume. Indeed, this energy allows the calculation of the seal mechanical properties. As a remark, the potential energy is given in J .

3 Evolution of the ferrofluid seal shape

As stated previously, the ferrofluid seal shape is directly linked to the magnetic field produced by the ring permanent magnets. We present in this section the evolution of ferrofluid seal shapes with three ring permanent magnets, as shown in Fig 1-A when one ring permanent magnet varies in height. The height variation of the middle ring permanent magnet can generate the formation of one or two ferrofluid seals. According to the intended application,

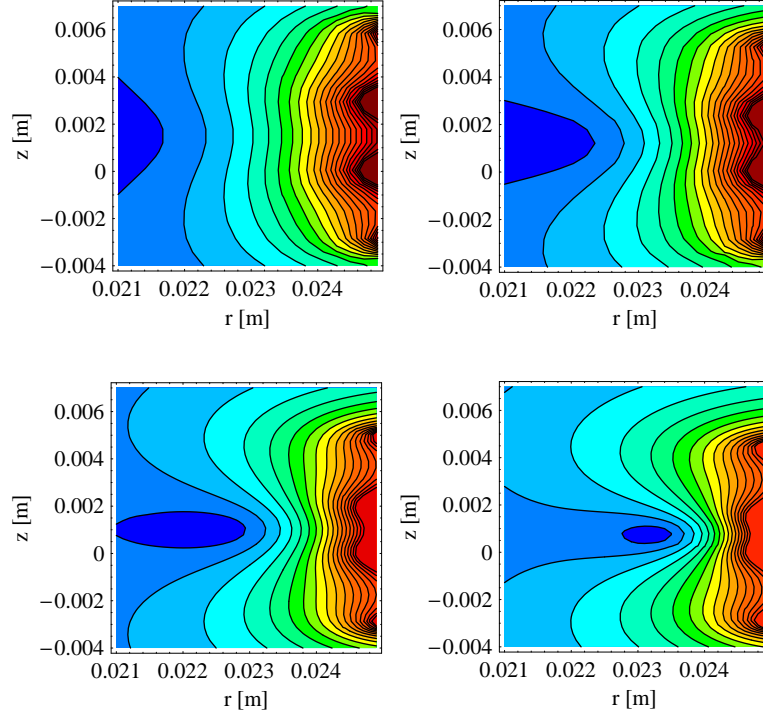


Fig. 4. Three magnet structure. Iso-pressure lines in front of the inner side of the magnets for increasing height of the middle magnet. The ferrofluid goes first to the dark red areas. For increasing volumes of the ferrofluid, the seal grows and fills then the areas from the warm to the cold colors.

the quantity of ferrofluid used and the ring permanent magnet dimensions must be optimized carefully. Let us consider the first configuration considered in this paper shown in Fig 1-A. The height of the ring permanent magnet located between the two ring permanent magnets whose polarizations are directed towards the inner piston has a great influence. We can see that by taking respectively the following dimensions for this ring permanent magnet: $h = 0.003$ m, $h = 0.0025$ m, $h = 0.002$ m, $h = 0.0015$ m though the upper and lower ring permanent magnets have the same height ($h = 0.003$ m). We represent in Fig 4 the growing ferrofluid seals with the two previous configurations in which the ring height varies.

Fig 4 demonstrates that we can have either one or two ferrofluid seals according to the choice of the ring permanent magnet dimensions. In addition, for a given quantity of ferrofluid, we can also have one or two ferrofluid seals, as shown in Fig 4. Some applications require two ferrofluid seals (ironless loudspeakers, ironless bearings) while other applications require one ferrofluid seal (small loudspeakers (tweeters)). Consequently, under magnetic fields which saturate totally the ferrofluid, the design of a ferrofluid seal depends on magnetic considerations only. Moreover, the magnetic properties of the device must be optimized essentially according to the ring permanent magnet dimensions and the quantity of ferrofluid used.

3.1 Describing a ferrofluid seal by mathematical means

The equations governing the magnetic pressure of the ferrofluid seal are rather complicated. Obtaining an accurate value of the ferrofluid seal volume is thus very difficult. However, this element of information is very useful for people involved in the design of ironless structures made of permanent magnets and ferrofluid seals. For example, if we consider the case of two ring permanent magnets whose polarizations are radial and in opposed directions, as shown in Fig 1-B, the shape of the ferrofluid seal between $r = 0.0246$ m and $r = 0.025$ m can be approximated as half an ellipse. Consequently, when the ferrofluid seal thickness is smaller than 0.0004 m, its contour can be written in terms of an equation of an ellipse (3).

$$\frac{(r - r_i)^2}{a_i^2} + \frac{z^2}{b_i^2} = 1 \quad (3)$$

Ellipse	a_i	b_i	r_i	error
5% E	0.00025	0.000275	0.025	0.5%
10% E	0.00027	0.000297	0.025	0.9%
15% E	0.00029	0.000319	0.025	1.4%

Table 1

Parameters of the equations of an ellipse describing small ferrofluid seals

To illustrate (3), Table (1) gives the parameters of the equations of ellipse describing the ferrofluid seal in Fig.4 for r between 0.0246 m and 0.025 m. We denote E , the quantity of magnetic energy of the volume of ferrofluid between 0.0246 m and 0.025 m. The approximation error between the equations of ellipse and the real contour shape of the ferrofluid seal is also given. When some ferrofluid is added, the shape of the ferrofluid seal changes and for $r < 0.0246$ m, the ferrofluid seal contour cannot be represented in terms of an equation of ellipse. Furthermore, we can point out that if a large amount of ferrofluid is added, the ferrofluid seal size becomes very large because of the magnet edge effects. In our configuration, the thickness of the ferrofluid seal for which the shape changes is 0.0006 m. This element of information is very important since it gives clearly what quantity of ferrofluid should be used to make a small seal.

3.2 *Shape of the crushed ferrofluid seal*

We take now the non-magnetic cylinder into account. The device has to be dimensioned in such a way that the cylinder crushes the seal, in order to reach the intended watertightness. Figure 5 shows where the ferrofluid goes when

Displacement	Energy reduction
0,1 mm	13%
0,15 mm	35%
0,2 mm	68%

Table 2

The energy reduction is a function of the radial displacement of the inner cylinder

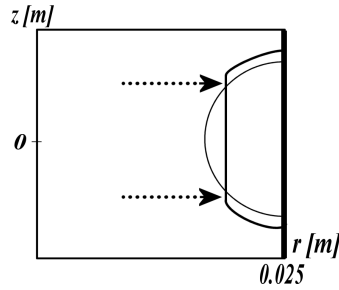


Fig. 5. Ferrofluid seal which is crushed

the inner non-magnetic cylinder crushes the ferrofluid seal. The phenomenon is axisymmetrical, as the inner cylinder is supposed here to be centered. As seen in Fig. 4, for small quantities of ferrofluid, the ferrofluid seal contour can be described in terms of an equation of ellipse. Therefore, when a small ferrofluid seal is crushed, the quantity of ferrofluid goes symmetrically under and above the initial ferrofluid seal by describing an equation of ellipse. This ellipse is truncated because of the inner non-magnetic cylinder. The change in the ferrofluid seal shape generates an energy reduction. Table 2 presents the energy reduction when the cylinder crushes radially the ferrofluid seal. The energy reduction is very important (68%) when the radial displacement of the inner cylinder is 0.0002 m.

4 Obtaining the static capacity of the ferrofluid seal

The calculation of the static capacity of a ferrofluid seal is useful for the design of watertightness seals. We present in this section a simple method for calculating this static capacity. Then, we present some optimized structures that ensure a good static capacity. We will see that the main criterion for the design of watertightness seals is both the thickness of the ferrofluid composing the seal and the ring permanent magnet dimensions.

4.1 *Using the magnetic potential energy*

In some applications as in ironless loudspeakers, the pressure underneath the non-magnetic cylinder can be very different from the pressure above the non-magnetic cylinder. Consequently, a pressure gradient appears and the ferrofluid seal is thus deformed. Therefore, the calculation of the ferrofluid seal capacity is required. For this purpose, a second configuration is considered, which corresponds to the case when a cylindrical air gap appears in the seal along the cylinder because of an applied pressure on one side of the seal. This case is realistic because this is especially near the non-magnetic cylinder that a perforation can appear due to a pressure gradient. We present in Fig 6-A a structure with three ring permanent magnets and two perforated ferrofluid seals and in 6-B a structure with two ring permanent magnets and one perforated ferrofluid seal. Let us consider the configuration shown in Fig 6-B. Two steps are necessary to determine the capacity of the ferrofluid seal. The first step is the determination of the potential energy of the ferrofluid seal without any perforation in the seal. To do so, a numerical integration of (2) leads to a first

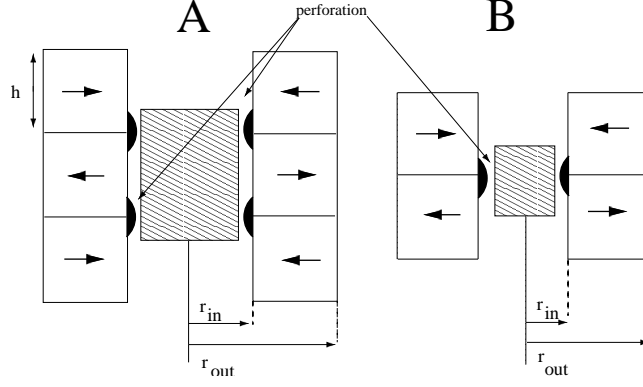


Fig. 6. Geometry: two ring permanent magnets and an inner non-magnetic cylinder; air gap in the seal

value of the potential energy which is denoted $E_m(1)$. The used numerical method is the GaussKronrod method. The second step is the determination of the potential energy of the ferrofluid seal with the perforation. Again, a numerical integration leads to a second value of the potential energy denoted $E_m(2)$. The energy difference is denoted ΔE_m and verifies (4):

$$\Delta E_m = E_m(1) - E_m(2) \quad (4)$$

The energy difference corresponds to the pressure work $\delta W(P)$ and satisfies (5):

$$\Delta E_m = \delta W(P) = P S d \quad (5)$$

where S is the surface area of the air gap and d is the thickness of the perforation. Consequently, the capacity P_{lim} verifies (6):

$$P_{lim} = \frac{\delta W(P)}{S d} \quad (6)$$

A numerical application has been done with several ring inner radii (Fig.7). We define the ferrofluid thickness as the thickness of the ferrofluid between

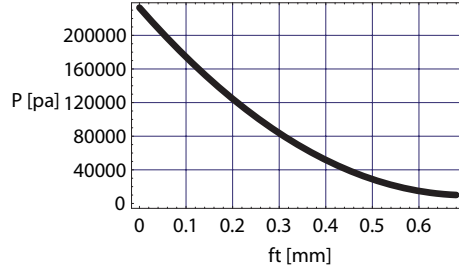


Fig. 7. The static limit pressure P [Pa] is a function of the ferrofluid seal thickness ft [mm]

Ferrofluid thickness	Volume	Hlim
0,1 mm	$4.7 \cdot 10^{-9} \text{ m}^3$	700 000 A/m
0,3 mm	$2.1 \cdot 10^{-8} \text{ m}^3$	600 000 A/m
0,5 mm	$1.2 \cdot 10^{-8} \text{ m}^3$	450 000 A/m

Table 3

Volume and Magnetic field corresponding to a given ferrofluid thickness the outer ring permanent magnets and the inner cylinder. Figure 7 shows that the thinner the ferrofluid seal is, the higher the pressure gradient to which the ferrofluid seal can resist is. Table 4.1 gives both the volume corresponding to each ferrofluid thickness and the smallest magnetic field $Hlim$ in the concerned volume.

5 Improving the static capacity of a ferrofluid seal

The previous section has presented a simple method for calculating the static capacity of a ferrofluid seal. For given ring permanent magnet dimensions, the ferrofluid seal thickness must be as thin as possible. Let us now consider the reciprocal problem in which the ferrofluid thickness is given and cannot

be changed. How can we improve and optimize its capacity ? The only way of changing the magnetic potential energy in the ferrofluid seal is to change the ring permanent magnet dimensions. However, the cost of the permanent magnet manufacturing must be taken into account as well as the structure dimensions required.

5.1 Optimizing the ring permanent magnet dimensions

Let us consider the two ring permanent magnets studied previously. The ferrofluid seal capacity can be improved by enhancing the magnetic potential energy inside it. As this magnetic potential energy is directly linked to the magnetic field produced by the ring permanent magnets, we can optimize the ring permanent magnets for improving the magnetic field in front of the ring permanent magnets. Strictly speaking, by extending the ring permanent magnet width, the magnetic field in the air gap increases. This phenomenon can be explained by using the Coulombian analogy. According to this analogy, the magnetic charges located on the outer faces of the ring permanent magnets reduce the magnetic field in the air gap. However, there is another way of improving the magnetic field in this air gap. To see that, let us consider two ring permanent magnets radially magnetized with increasing heights. We take $h = 0.002$ m, $h = 0.0025$ m , $h = 0.003$ m, $h = 0.0035$ m, $h = 0.004$ m and $h = 0.0045$ m respectively and we plot the magnetic field generated by the two ring permanent magnets. We represent in Fig 8 the six configurations. Figure 8 clearly shows that the longer the ring permanent magnet heights are, the stronger the magnetic field in the air gap is. However, as shown in Fig 8, the ferrofluid seal decreases in height when the ring permanent magnet heights

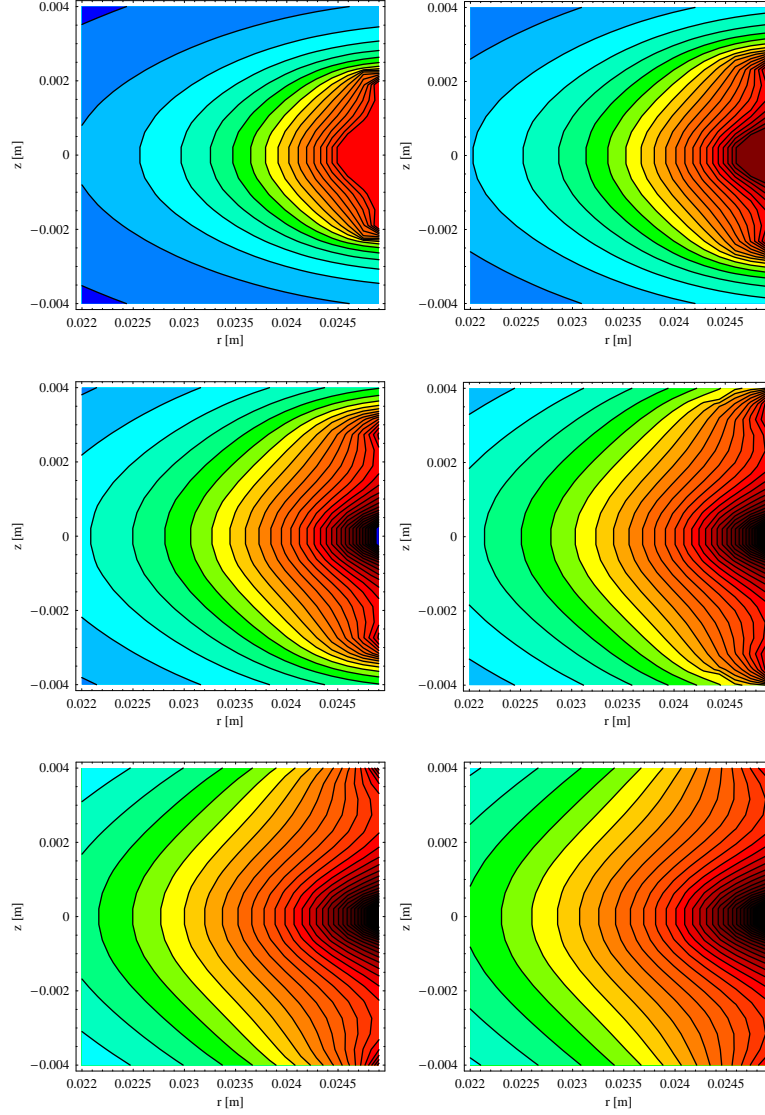


Fig. 8. Representation of growing ferrofluid volumes under magnetic fields when the ring permanent magnet heights increase; $h = 0.002$ m (top-left), $h = 0.0025$ m (top-right), $h = 0.003$ m (middle-left), $h = 0.0035$ m (middle-right), $h = 0.004$ m (down-left), $h = 0.0045$ m (down-right). For each ring permanent magnet, the radial width equals 0.003 m and $J = 1$ T.

increase. This implies that for a structure that requires a small ferrofluid seal with the greatest static capacity, the height of the ring permanent magnets must be greater than their radial widths.

5.2 Discussion about the way of improving the static capacity of a ferrofluid seal

The previous sections have shown that there were two ways of improving the static capacity of a ferrofluid seal for a given ferrofluid thickness. The first way of improving the ferrofluid seal static capacity is to improve the ring permanent magnet radial widths. Indeed, the magnetic field produced by a permanent magnet results from the contributions of positive magnetic charge surface densities and negative magnetic charge surface densities. The sum of these contributions give the magnetic field value in a point in space. For cylindrical geometries in which we look for optimizing the magnetic field in front of one ring permanent magnet face, the contribution of the fictitious magnetic charge surface densities located on the opposite face (outer face) must be as small as possible. The only way of reducing the weight of these latter magnetic charges is to increase the radial width of the ring permanent magnets. It is to be noted that this is generally the way the passive magnetic bearings are optimized.

The second way of improving the ferrofluid seal static capacity is to change the ring permanent magnet heights. However, such an optimization is a little bit more complicated because it must be done according to the radial width of the ring permanent magnets. When the ring permanent magnet heights are small compared to their radial widths, the ferrofluid has a low magnetic potential energy and can be easily perfored.

6 Conclusion

This paper has presented an analytical method to design ironless structures composed of ring permanent magnets and ferrofluid seals. This way of designing such structures is possible because all the configurations considered are ironless. Moreover, the ferrofluid is submitted to a magnetic field which totally saturates it. Consequently, most of the terms in the Bernoulli equation describing the state of the ferrofluid can be omitted because they do not play a key role in the static behavior of the seal. The concept of potential magnetic energy is useful because it leads to simple calculations of the mechanical properties of ferrofluid seals. With the assumptions taken in this paper, this potential magnetic energy is linked to the interaction between the magnetic field created by the ring permanent magnets and the ferromagnetic particles that constitute the ferrofluid seal. Numerous approaches exist but are not always suitable for optimization purposes. The authors feel that this way of modelling ferrofluid seals is suitable for improving the capacity of the seal or for optimizing the quantity of ferrofluid that should be used in a seal. In any case, the accurate calculation of the energy in a ferrofluid seal is difficult to perform because the weak contributions of the terms omitted in the Bernoulli equation generate also energetic terms. However, some optimizations can be performed only with the analytical expressions of the magnetic field produced by the ring permanent magnets. The variation in height in some of them has a great influence on the ferrofluid seal shape as well as its magnetic potential energy. Finally, this paper has presented a method for improving the ferrofluid seal static capacity. The ring permanent magnet height plays a key role in the optimization of the ferrofluid seal capacity. The more the ring permanent

magnet heights are important compared to their radial widths, the more the magnetic potential energy in a given volume of ferrofluid seal is important. Such results can be used either for the design of ironless loudspeaker structures or for the manufacturing of ironless bearings.

References

- [1] R. E. Rosensweig, *Ferrohydrodynamics*. Dover, 1997.
- [2] C. Holm and J. J. Weiss, “The structure of ferrofluids : A status report,” *Current Opinion in colloid and interface science*, vol. 10, no. 4, pp. 133–140, 2005.
- [3] Y. L. Raikher, V. I. Stepanov, J. C. Bacri, and R. Perzynski, “Orientational dynamics in magnetic fluids under strong coupling of external and internal relaxations,” *Journal of Magnetism and Magnetic Materials*, vol. 289, pp. 222–225, 2005.
- [4] H. S. Lee and I. Nakatani, “On the chemical stability of iron-nitride magnetic fluids in atmospheric conditions,” *Journal of Magnetism and Magnetic Materials*, vol. 201, pp. 23–26, 1999.
- [5] G. S. Park and S. H. Park, “Determination of the curvature of the magnetic fluid under external forces,” *IEEE Transactions on Magnetics*, vol. 38, pp. 957–960, march 2002.
- [6] Z. Meng and Z. Jibin, “An analysis on the magnetic fluid seal capacity,” *Journal of Magnetism and Magnetic Materials*, vol. 303, pp. e428–e431, 2006.
- [7] K. Raj, V. Moskowitz, and R. Casciari, “Advances in ferrofluid in ferrofluid technology,” *Journal of Magnetism and Magnetic Materials*, vol. 149, pp. 174–180, 1995.

- [8] G. Lemarquand, “Ironless loudspeakers,” *IEEE Trans. Magn.*, vol. 43, no. 8, pp. 3371–3374, 2007.
- [9] M. Berkouk, V. Lemarquand, and G. Lemarquand, “Analytical calculation of ironless loudspeaker motors,” *IEEE Trans. Magn.*, vol. 37, no. 2, pp. 1011–1014, 2001.
- [10] R. Ravaud, G. Lemarquand, V. Lemarquand, and C. Depollier, “Ironless loudspeakers with ferrofluid seals,” *Archives of Acoustics*, vol. 33, no. 4, pp. 3–10, 2008.
- [11] R. Ravaud and G. Lemarquand, “Modelling an ironless loudspeaker by using three-dimensional analytical approaches,” *Progress in Electromagnetics Research, PIER 91*, pp. 53–68, 2009.
- [12] R. Ravaud and G. Lemarquand, “Design of ironless loudspeakers with ferrofluid seals: analytical study based on the coulombian model,” *Progress in Electromagnetics Research B*, vol. 14, pp. 285–309, 2009.
- [13] G. S. Park and K. Seo, “New design of the magnetic fluid linear pump to reduce the discontinuities of the pumping forces,” *IEEE Trans. Magn.*, vol. 40, pp. 916–919, 2004.
- [14] I. Tarapov, “Movement of a magnetizable fluid in lubricating layer of a cylindrical bearing,” *Magnetohydrodynamics*, vol. 8, no. 4, pp. 444–448, 1972.
- [15] J. Walker and J. Backmaster, “Ferrohydrodynamics thrust bearings,” *Int. J. Eng. Sci.*, vol. 17, pp. 1171–1182, 1979.
- [16] N. Tiperi, “Overall characteristics of bearings lubricated ferrofluids,” *ASME J. Lubr. Technol.*, vol. 105, pp. 466–475, 1983.
- [17] S. Miyake and S. Takahashi, “Sliding bearing lubricated with ferromagnetic fluid,” *ASLE Trans.*, vol. 28, pp. 461–466, 1985.

- [18] H. Chang, C. Chi, and P. Zhao, "A theoretical and experimental study of ferrofluid lubricated four-pocket journal bearing," *Journal of Magnetism and Magnetic Materials*, vol. 65, pp. 372–374, 1987.
- [19] Y. Zhang, "Static characteristics of magnetized journal bearing lubricated with ferrofluids," *ASME J. Tribol.*, vol. 113, pp. 533–538, 1991.
- [20] T. Osman, G. Nada, and Z. Safar, "Static and dynamic characteristics of magnetized journal bearings lubricated with ferrofluid," *Tribology International*, vol. 34, pp. 369–380, 2001.
- [21] R. C. Shah and M. Bhat, "Anisotropic permeable porous facing and slip velocity squeeze film in axially undefined journal bearing with ferrofluid lubricant," *Journal of Magnetism and Magnetic Materials*, vol. 279, pp. 224–230, 2004.
- [22] F. Cunha and H. Couto, "A new boundary integral formulation to describe three-dimensional motions of interfaces between magnetic fluids," *Applied mathematics and computation*, vol. 199, pp. 70–83, 2008.
- [23] Q. Zhang, S. Chen, S. Winoto, and E. Ong, "Design of high-speed magnetic fluid bearing spindle motor," *IEEE Trans. Magn.*, vol. 37, no. 4, pp. 2647–2650, 2001.
- [24] R. C. Shah and M. Bhat, "Ferrofluid squeeze film in a long bearing," *Tribology International*, vol. 37, pp. 441–446, 2004.
- [25] S. Chen, Q. Zhang, H. Chong, T. Komatsu, and C. Kang, "Some design and prototyping issues on a 20 krpm hdd spindle motor with a ferro-fluid bearing system," *IEEE Trans. Magn.*, vol. 37, no. 2, pp. 805–809, 2001.
- [26] M. Miwa, H. Harita, T. Nishigami, R. Kaneko, and H. Unozawa, "Frequency characteristics of stiffness and damping effect of a ferrofluid bearing," *Tribology Letter*, vol. 15, no. 2, pp. 97–105, 2003.
- [27] W. Ochonski, "The attraction of ferrofluid bearings," *Mach. Des.*, vol. 77, no. 21, pp. 96–102, 2005.

- [28] R. Ravaud, G. Lemarquand, V. Lemarquand, and C. Depollier, “The three exact components of the magnetic field created by a radially magnetized tile permanent magnet.,” *Progress in Electromagnetics Research, PIER 88*, pp. 307–319, 2008.
- [29] G. Matthies and U. Tobiska, “Numerical simulation of normal-field instability in the static and dynamic case,” *Journal of Magnetism and Magnetic Materials*, vol. 289, pp. 436–439, 2005.
- [30] A. Ivanov, S. Kantorovich, V. Mendelev, and E. Pyanzina, “Ferrofluid aggregation in chains under the influence of a magnetic field,” *Journal of Magnetism and Magnetic Materials*, vol. 300, pp. e206–e209, 2006.
- [31] R. Ravaud, G. Lemarquand, V. Lemarquand, and C. Depollier, “Analytical calculation of the magnetic field created by permanent-magnet rings,” *IEEE Trans. Magn.*, vol. 44, no. 8, pp. 1982–1989, 2008.